Available online at www.sciencedirect.com
SCIENCE DIRECT®
Journal of Power Sources 125 (2004) 149–154
JOURNAL OF POWER SOURCES
www.elsevier.com/locate/jpowsour

Electrochemical properties of LSM–CBO composite cathode

Hui Zhao*, Lihua Huo, Shan Gao

College of Chemistry and Chemical Technology, Heilongjiang University, Harbin 150080, PR China

Received 11 April 2003; received in revised form 25 July 2003; accepted 30 July 2003

Abstract

In order to develop a cathode that can be used in intermediate temperature solid oxide fuel cells (ITSOFC), the composite materials $La_{0.8}Sr_{0.2}MnO_3$–$Ce_{0.7}Bi_{0.3}O_2$ (LSM–CBO) has been prepared and its electrode performances are investigated below 700 °C by AC impedance spectroscopy and dc polarization measurements. Results indicate that the oxygen adsorption process is the reaction rate limiting step. The polarization resistance decreases with the increasing of CBO contents. The optimum value of 50 wt.% CBO in LSM results in 1.78 $\Omega\,cm^2$ area specific resistivity (ASR), which indicates that the LSM–CBO composite electrode is a promising cathode material in ITSOFC.

Keywords: LSM–CBO; Composite cathode; ITSOFC

1. Introduction

As we know, one of the major problem encountered today to develop ITSOFC is the large cathode overpotential caused by the reduced operation temperature. It is reported, for example, that the polarization resistance of $La_{0.8}Sr_{0.2}MnO_3$ (LSM) increases dramatically from 1 $\Omega\,cm^{-2}$ at 1000 °C to 2000 $\Omega\,cm^{-2}$ at 500 °C [1]. So it is interesting to find alternative materials that can be used in ITSOFC. Now days, two trends have been developed to overcome this problem. One way is to find mixed conducting materials, such as LSCF [2–4], which has shown improved cathode properties, due to the rapid surface exchange kinetics, high oxygen vacancy concentration, and the extended triple phase boundary (TPB) from the electrolyte/electrode interface to the bulk of the electrode [2,5–7]. Another way is to form composite electrode [8]. Generally, a high electron-conducting phase is mixed together with a highly ionic conducting phase [9–13]. It is believed that the cathode properties can be improved by the increasing of TPB formed on the electrolyte/electrode interface. For this purpose, the ionic conducting material should have high conductivity at low temperature. Studies have shown that LSM–CGO composite electrode always exhibited improved performance than that of LSM–YSZ, due to the much higher oxygen ionic conductivity of CGO at low temperature.

Although LSM–CGO composite cathode has exhibited much improved catalysis properties, searching alternative materials is still attractive. Bismuth doped materials have been investigated recently as possible cathode materials in ITSOFC [14]. In the previous study, bismuth doped ceria has shown high oxygen ionic conductivity [15–18]. For example, the conductivity of $Ce_{0.7}Bi_{0.3}O_2$ (here after we refer it as CBO) is 0.014 S cm^{-2} at 600 °C [15], comparable to that of CGO under the same temperature. It is interesting to study the LSM–CBO composite material and its possible usage in ITSOFC. Here we report the $La_{0.8}Sr_{0.2}MnO_3$–$Ce_{0.7}Bi_{0.3}O_2$ composite electrode and its cathode properties below 700 °C.

2. Experimental

YSZ powders (TZ8Y, Tosoh Co.) are used to prepare the electrolyte pellet. The powders are pressed uniaxially at 350 MPa to form green pellet. Sintering is carried out at 1450 °C for 4 h. The density of the obtained pellet is determined by Archimedes' method, and it is over 95% of the theoretical value. Both sides of the pellet are roughed with 240# SiC grit paper and then cleaned by ultrasonic. The $Ce_{0.7}Bi_{0.3}O_2$ powders are prepared according to Ref. [15]. The LSM powders are supplied by Seattle Specialty Ceramics, Inc. The electrode slurry is made with desired amount of LSM and CBO together with ethylene glycol and ball milled overnight. The compositions of the slurry are varied from 10 to 60 wt.% of CBO. The slurry is painted with brush on one side of the YSZ pellet. Platinum paste (Engelhard,

* Corresponding author.
E-mail address: zhaohui98@yahoo.com (H. Zhao).

0378-7753/$ – see front matter © 2003 Elsevier B.V. All rights reserved.
doi:10.1016/j.jpowsour.2003.07.009

Cat. No. 6082) is painted on the other side in symmetric configuration. Pt wire is used as reference electrode and put on the same side that of the working electrode. The cell is first heated up to 500 °C to eliminate the organic binders, and then to the desired temperatures for 4 h. The structure and phase stability of the composite materials are characterized by powder X-ray diffraction on a Siemens D5005 diffractometer. The scan rate was 0.1° (2θ) min^{-1}. The impedance spectrum is recorded over the frequency range 1 MHz–0.01 Hz using autolab PGStat30. The measurement is performed in the temperature range 500–700 °C. The obtained data is analysis with Z-view software. The dc polarization experiment is performed by chronoampermetry method [19], which involves a potential step followed by recording the current density as a function of time. The cathode overpotential is calculated according to the following equation:

$$\eta_{WE} = \Delta U_{WR} - iR_{el} \quad (1)$$

where η_{WE} represents the cathode overpotential, ΔU_{WR} is the applied voltage between working electrode and reference electrode, i is the current density flowing through the test cell and R_{el} is the resistance of the electrolyte obtained from impedance spectrum.

3. Results and discussions

It is reported that LSM can react with YSZ to form insulator phase $La_2Zr_2O_7$, which in turn has negative effect on the electrochemical properties of LSM–YSZ composite cathode. So it is necessary first to know the reactivity of LSM with the bismuth doped ceria compound. Fig. 1 gives the XRD pattern of LSM–CBO composite materials that has been treated under different experimental conditions. It is observed that the initial mixed powders give the typical XRD patterns coming from LSM and CBO solid solution.

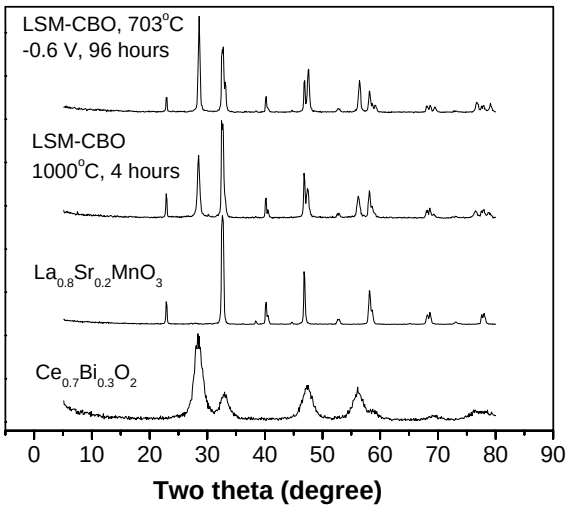

Fig. 1. XRD spectrum of LSM–CBO composite materials sintered under different experimental conditions.

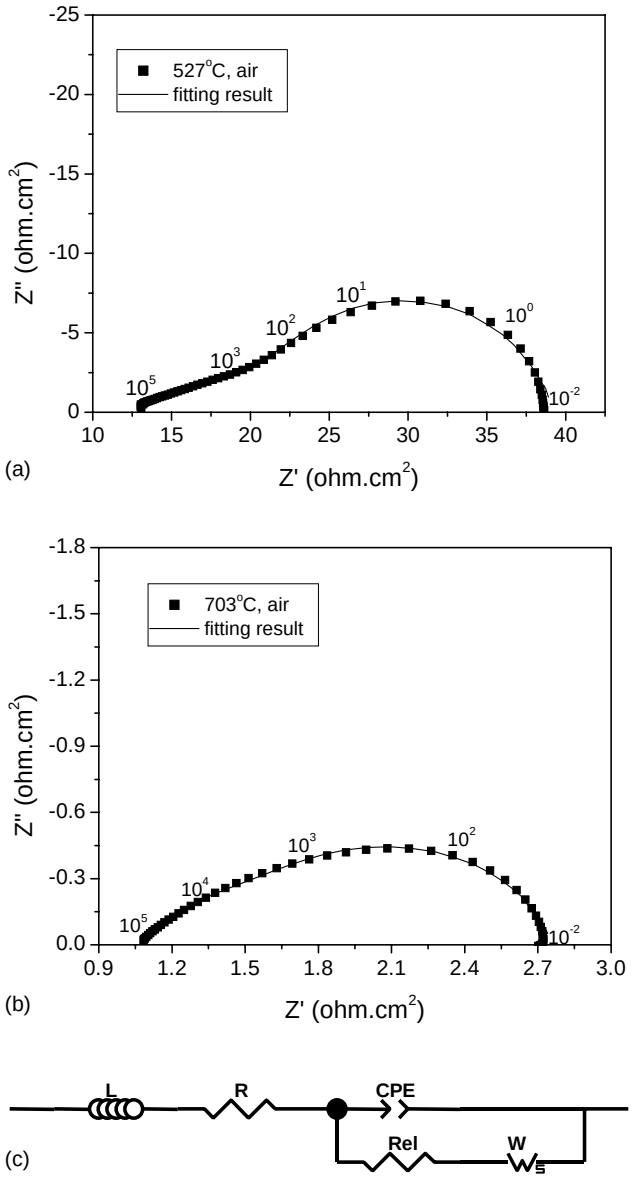

Fig. 2. Nyquist plot of LSM–CBO (50 wt.%) composite electrode on YSZ pellets measured at (a) 527 °C, and (b) 703 °C, respectively in air, (c) equivalent circuit, $LR(CPE(R_{el}W))$.

No other phases are observed after the mixture was heated at 1000 °C for 4 h, or at the measurement temperature 703 °C and under 0.6 V cathode potential for 96 h. It is therefore concluded that the mixed LSM and CBO composite material is stable under the experimental conditions.

Fig. 2a shows the typical Nyquist plot of LSM–CBO composite electrode on YSZ pellets measured at 527 °C in air. There are two depressed arcs that can be observed. The first arc is relatively small, the second one is dominated in the whole measurement temperature range. The corresponding relaxation frequencies at 527 °C are about 1 kHz and 5 Hz, respectively. As the temperature increases, the impedance of the two arcs decreases, and at 700 °C (see Fig. 2b), the contributions of the two arcs cannot be clearly distinguished. In

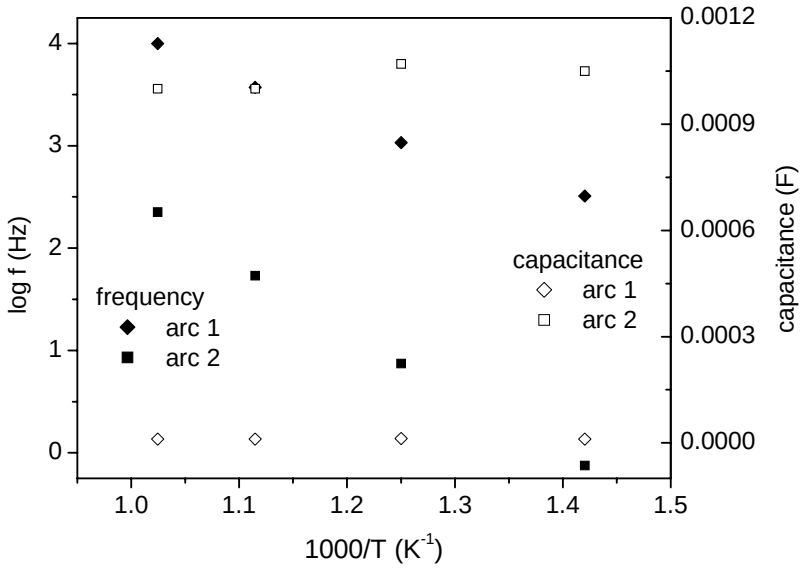

Fig. 3. The plots of the relaxation frequency and the corresponding capacitances with temperatures.

order to separate the contributions of the two arcs, a equivalent circuit, $LR(\mathrm{CPE}(R_{\mathrm{el}}W))$ [20], is used to fit the data (Fig. 2c). The fitting results are also shown in Fig. 2. Here L represents the inductance caused by the device and the connect leads, R is the resistance of YSZ electrolyte. The remaining components represent the total polarization resistance. R_{el} corresponds to the contribution of the first arc located at high frequency side, W represents a Warburg element, which is related to the arc located in the lower frequency side. The second arc is not likely due to the gas diffusion resistance, because the amplitude of this arc decreases with increasing temperature. It is 17.8 $\Omega\,\mathrm{cm}^{-2}$ at 527 °C and 1.2 $\Omega\,\mathrm{cm}^{-2}$ at 703 °C, respectively, noting that the gas diffusion resistance does not depend on the temperature [21].

Fig. 3 plots the relaxation frequency and the corresponding capacitances against temperatures. This kind of plot has been used before to study different contributions of the test cell [22]. It is observed that the relaxation frequency of the two arcs increases linearly with the increase of temperature. The corresponding capacitance remains unchanged. The calculated values of the capacitance associated with the two arcs are about 1×10^{-5} and 1×10^{-3} F, respectively, consistent with electrochemical reaction mechanism that occurred on electrode [23]. These results further prove that two arcs exist in the impedance spectrum, and they represent two different electrochemical processes occurred on electrode. In order to investigate the effect of sintering temperature on the LSM–CBO cathode properties, a number of different sintering conditions are studied. Fig. 4 gives the Nyquist plot of the composite cathodes sintering at different temperatures for 4 h and then measured at 703 °C in air. From the impedance spectrum, we observe that the total polarization resistance is relatively large when the electrode is sintered at 800 °C. Although the major contribution still comes from the second arc, the amplitude of the first arc increases dramatically. We propose it is due to the low sintering temperatures and therefore the bad contact between the LSM and CBO particles and the electrode/electrolyte interface. The similar phenomena have been observed before in the investigation of LSM–YSZ composite cathode [24]. When the sintering temperature is 900 °C, the total polarization resistance is reduced. Considering the low melting point of Bi_2O_3 doped CBO powders, we believe that at this temperature, a good contact has been formed between CBO and LSM particles, which in turn will reduce the grain boundary resistance in large extent. When the sintering temperature is up to 1000 °C, however, the polarization resistance increases again. We believe that it is due to the over-sintering of LSM–CBO composite electrode. In this case, the nano-size CBO powder [15] is used, which may melt and cover the surface of LSM powders at 1000 °C,

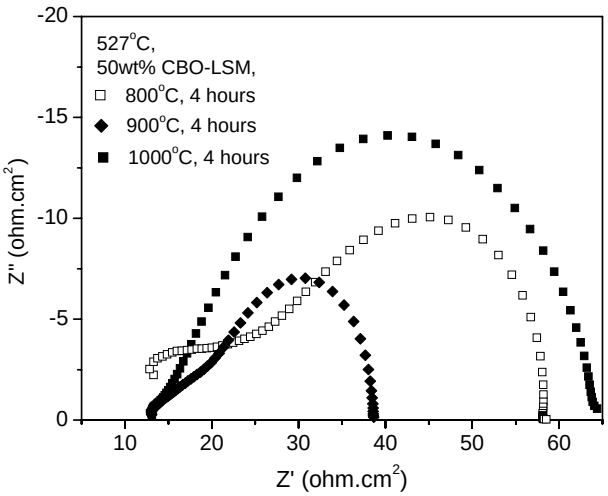

Fig. 4. Nyquist plot of the composite cathodes sintering at different temperatures for 4 h and then measured at 527 °C in air.

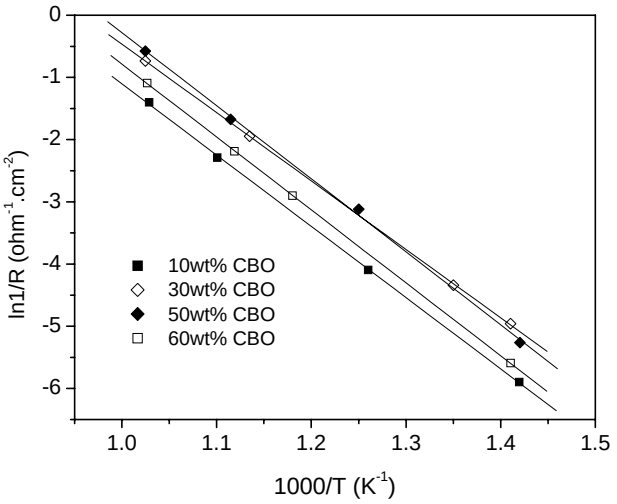

Fig. 5. The Arrhenius plot of the total polarization resistance of the cathode materials with different compositions.

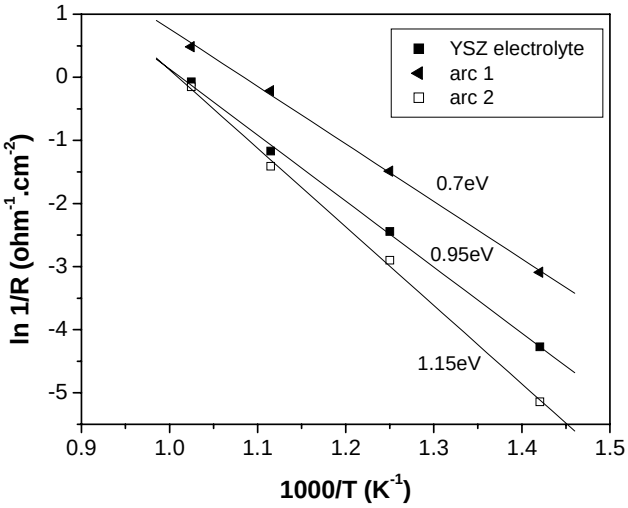

Fig. 6. The Arrhenius plot of electrolyte and electrode polarization resistances for 50 wt.% CBO–LSM composite cathode measured in air.

and the TPB in LSM–CBO composite cathode will be decreased. The similar effects have also been observed in the reported LSM–YSZ and LSM–CGO composite materials [22,24]. Hereafter all the studied electrodes were sintered at 900 °C for 4 h to obtain the best sintering performance.

Fig. 5 shows the total polarization resistance (given by the difference between the real-axis intercepts of the impedance spectrum) versus measurement temperatures for different composite cathodes. It is observed that the total polarization resistance decreases with the increase of CBO contents, the optimum composition is around 30–50 wt.% CBO in LSM powders, which is roughly in agreement with the estimated values based on the effective medium percolation theory [25–27]. In fact, we observe that the lowest cathode polarization resistance is obtained in the mixture of 50 wt.% CBO and 50 wt.% LSM. But the difference between 30 and 50 wt.% mixed CBO composite electrodes is small, which can be considered as the cathode-to-cathode data scattering in the measurements, as that reported in the study of LSCF–CGO composite cathode [28]. Therefore in the below experiments, only the optimum composite electrodes (with 50 wt.% CBO and sintering at 900 °C for 4 h) are further studied.

Fig. 6 shows the temperature dependence of electrolyte and electrode polarization resistances measured in air. Straight lines are obtained for all the plots. The activation energy of YSZ electrolyte is 0.9 eV, in agreement with the reported values [2]. The activation energy for the first arc is small, about 0.7 eV. In the previous study, it is found that the activation energy for grain boundary contribution in CBO is about 1 eV [15], so it seems that in this experiment, the first arc is not due to the grain boundary contribution. Considering the capacitance value (10^{-5} F) of the first arc, it maybe related to the charge transfer processes occurred on the LSM/CBO interface, which is similar as that observed in the LSCF–CGO composite electrode [2,12]. The activation energy for the second arc is relatively large. It is 1.15 eV. This value is in good agreement with the reported values for LSM–YSZ and LSM–CGO (1.2 eV) [21] composite materials.

The dependence of polarization resistance on oxygen partial pressure is shown in Fig. 7. It is observed that the first arc shows little dependence on oxygen partial pressure, and the second arc exhibits small dependence on P_{O_2}. If we plot $\log(R_p)$ against $(P_{O_2})^{-m}$, we obtain that m is 0.1 for the first arc, and 0.26 for the second arc. The value for the second arc is quite similar to that of LSM–YSZ [29] (there is no report value for LSM–CGO), but different from LSCF–CGO cathode [28]. In general, the $P_{O_2}^{1/4}$ dependence is attributed to the charge transfer process, when the corresponding double layer capacitance is observed. In our case, the value of the capacitance is about 1 mF, which is too large to be

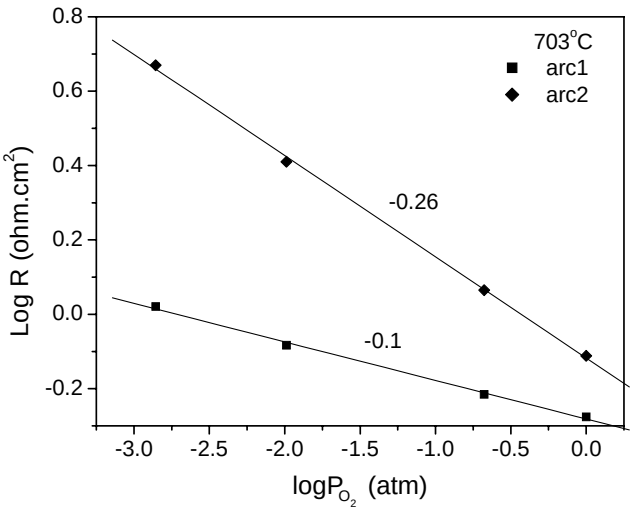

Fig. 7. The dependence of polarization resistance on oxygen partial pressure.

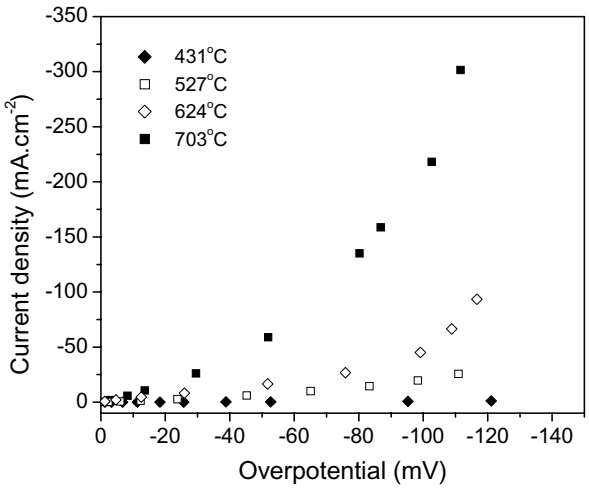

Fig. 8. The overpotential–current density curves measured at different temperatures in air.

associated with a double layer capacitance. This value is typical of an electrode "pseudo-capacitive" behavior [30]. We consider that this process is related to the non-Faraday phenomena occurred on the electrode. Considering the activation energy (1.15 eV in our case) and the weak oxygen partial pressure dependence ($m = 0.26$), we propose the process behaviors in the same rate limiting mechanism as that reported before for the LSM materials (the activation energy is about 1 eV, and the slope of P_{O_2} dependence curve is between 0 and 1/3) [31]. In that case, the oxygen adsorption process has been considered as the rate limiting step. Following the same argument, we propose that the adsorption process is the rate limiting step in our study. Fig. 8 shows the dc polarization curves measured at different temperatures in air. It is observed that the current increases with the measurement temperature and applied overpotential. As we known, when the concentration limiting process (such as dissociation and/or adsorption) becomes the rate limiting step, the modified Butler–Volmer expression should be used [32]. Under low cathodic overpotential, the current–overpotential curve follows the equation:

$$\eta = \frac{RT}{2F}\ln\left(\frac{1-I}{I_1}\right) \quad (2)$$

Here I_l is the limiting current [33]. From the derivative of η against I, we can obtain the area specific resistance. The value is compared to the deduced area specific resistance from the impedance spectrum (Table 1). We can see that both techniques give the similar values for the area specific resistance. The polarization resistance obtained at 700 °C is about 1.78 Ω cm^{-2}, close to that of LSM–CGO material [21]. This result is expectable, because CBO has been found to show high ionic conductivity below 700 °C. At present, we do not observe the limiting current plateau in the current–overpotential curve, due to the small overpotential applied in the study. Our results indicate that the formed LSM–CBO composite material can be considered as a possible cathode used in ITSOFC.

Table 1
Comparison of the area specific resistance obtained from the EIS measurement and from the inverse of the linear expression between 0 and −10 mV, respectively

Temperature (°C)	$\Delta\eta/\Delta i$ (Ω cm^{-2})[a]	R_p (Ω cm^{-2})[b]
431	184.5	193.2
527	21.4	22.6
621	5.41	5.34
703	1.62	1.78

[a] The polarization resistance was calculated from the linear part of the overpotential–current density curve.
[b] The polarization resistance was obtained from the EIS spectrum.

4. Conclusions

The $La_{0.8}Sr_{0.2}MnO_3$–$Ce_{0.7}Bi_{0.3}O_2$ composite material has been prepared and its cathode properties have been studied below 700 °C. The polarization resistance decreases with the addition of CBO in LSM. The lowest polarization resistance, 1.78 Ω cm^{-2} at 700 °C, is found in the 50 wt.% CBO composite electrode. Impedance analysis and oxygen partial pressure dependence study indicate that the oxygen adsorption process is the reaction rate limiting step. The electrode performance can be further improved by adjusting the microstructure to increase TPB, and therefore promote the oxygen adsorption reactions that occurred on the composite electrode.

Acknowledgements

We would like to thank the support from Natural Science Foundation of Heilongjiang Province and the Joint Research Fund for Oversea Scholars of Province.

References

[1] R. Doshi, V.L. Richards, J.D. Carter, X.P. Wang, M. Krumpelt, J. Electrochem. Soc. 146 (1999) 1273.
[2] S.B. Adler, J.A. Lane, B.C.H. Steele, J. Electrochem. Soc. 143 (1996) 3554.
[3] B.C.H. Steele, Solid State Ionics 75 (1995) 157.
[4] B.C.H. Steele, Solid State Ionics 86–88 (1996) 1223.
[5] C.C. Chen, M.M. Nasralla, H.U. Anderson, in: S.C. Singhal, H. Iwahara (Eds.), Proceedings of the Third International Symposium on the Solid Oxide Fuel Cells, The Electrochemical Society Proceedings Series, Pennington, NY, 1999, p. 252.
[6] L.-W. Tai, M.M. Nasrallah, H.U. Anderson, in: S.C. Singhal, H. Iwahara (Eds.), Proceedings of the Third International Symposium on the Solid Oxide Fuel Cells, The Electrochemical Society Proceedings Series, Pennington, NY, 1999, p. 241.
[7] C.C. Chen, M.M. Nasralla, H.U. Anderson, M.A. Alim, J. Electrochem. Soc. 142 (1995) 491.
[8] T. Kenjo, M. Nishiya, Solid State Ionics 57 (1992) 295.

[9] M.J.L. Ostergard, C. Clausen, C. Bagger, M. Mogensen, Electrochem. Acta 40 (1995) 1971.
[10] M. Juhl, S. Primdahl, C. Manon, M. Mogensen, J. Power Sources 61 (1996) 173.
[11] T. Tsai, S.A. Barnett, Solid State Ionics 93 (1997) 207.
[12] V. Dusastre, J.A. Kilner, Solid State Ionics 126 (1999) 163.
[13] C. Xia, F. Chen, M. Liu, Electrochem. Solid State Lett. A52 (2001) 4.
[14] H. Zhao, M. Pijolat, J. Mater. Chem. 12 (2002) 3787.
[15] H. Zhao, S. Feng, W. Xu, Mater. Res. Bull. 35 (2000) 2379.
[16] H. Zhao, S. Feng, Chem. Mater. 11 (1999) 958.
[17] G. Li, L. Li, S. Feng, M. Wang, L. Zhang, X. Yao, Adv. Mater. 11 (1999) 146.
[18] G. Li, Y. Mao, L. Li, S. Feng, M. Wang, X. Yao, Chem. Mater. 11 (1999) 1259.
[19] A. Espuirol, N. Brandon, N. Bonanos, J. Kilner, M. Mogensen, B.C.H. Steele, in: A.J. McEvoy (Ed.), Proceedings of the Fourth European Solid Oxide Fuel Cell Forum, U. Bossel, Oberrohrdorf, Switzerland, 2000, p. 225.
[20] S.R. Taylor, E. Gileadi, Corr. Sci. 51 (1995) 664.
[21] N.T. Hart, N.P. Brandon, M.J. Day, N. Lapena-Rey, J. Power Sources 106 (2002) 42.
[22] E.J.L. Schouler, N. Mesbahi, G. Vitter, Solid State Ionics 9/10 (1983) 989 (and reference therein).
[23] J.T.S. Irvine, D.C. Sinclair, A.R. West, Adv. Mater. 2 (1990) 132.
[24] M.J. Jørgensen, S. Primdahl, C. Bagger, M. Mogensen, Solid State Ionics 139 (2001) 1.
[25] B.C.H. Steele, Solid State Ionics 94 (1997) 239.
[26] D.S. Mclachlam, M. Blaszkiewicz, R.E. Newham, J. Am. Ceram. Soc. 73 (1990) 2187.
[27] S.W. Matin, Solid State Ionics 51 (1992) 19.
[28] E.P. Murray, M.J. Sever, S.A. Barnett, Solid State Ionics 148 (2002) 27.
[29] E.P. Murray, T. Tsai, S.A. Barnett, Solid State Ionics 110 (1998) 235.
[30] M. Kleitz, Solid State Ionics 3/4 (1984) 513.
[31] J.V. Herle, A.J. McEvoy, K.R. Thampi, Electrochim. Acta 41 (1996) 1447.
[32] D.Y. Wang, A.S. Nowick, J. Electrochem. Soc. 126 (1979) 1155.
[33] E. Siebert, A. Hammouche, M. Kleitz, Electrochim. Acta 40 (1995) 1741.